



Reactor Physics Benchmark of the First Criticality in the Molten Salt Reactor Experiment

Dan Shen,^a Germina Ilas,^b Jeffrey J. Powers,^b and Massimiliano Fratoni^{a*}

^a*University of California, Berkeley, California*

^b*Oak Ridge National Laboratory, Oak Ridge, Tennessee*

Received December 6, 2020

Accepted for Publication January 20, 2021

Abstract — *The deployment of molten salt reactors requires validation of the computational tools used to support the licensing process. The Molten Salt Reactor Experiment (MSRE), built and operated in the 1960s, offers a unique inventory of experimental data for reactor physics benchmarks. The first benchmark based on the MSRE appeared in “The 2019 Edition of the IRPhEP [International Reactor Physics Experiment Evaluation Project] Handbook.” The benchmark refers to the first criticality experiment at zero power, stationary salt, and uniform temperature with ^{235}U fuel. Simulations carried out for the developed benchmark model with the Monte Carlo code Serpent and ENDF/B-VII.1 cross-section library found that the calculated neutron multiplication is 1.02132 (± 3 pcm) and that the combined bias of the model and experimental uncertainty is below 500 pcm. Such discrepancy between the experimental and calculated k_{eff} is not uncommon in benchmarks for graphite-moderated systems. The model created through this effort paves the way to additional benchmarks targeting reactor physics quantities of interest beyond multiplication factor.*

Keywords — *Molten salt reactor, criticality, benchmark.*

Note — *Some figures may be in color only in the electronic version.*

I. INTRODUCTION

In recent years molten salt reactors (MSRs) have received worldwide attention from private and public entities seeking to commercialize such reactor concepts. A crucial step toward commercialization is to build confidence in the computational tools that are used not only to design these systems but also to prove their safety case. Benchmarks for validation of reactor physics codes are, arguably, the most challenging as they require critical facilities that are lengthy and costly to build. In this regard, the Molten Salt Reactor Experiment (MSRE), built and

operated at the Oak Ridge National Laboratory (ORNL) in the 1960s, offers a unique inventory of experimental data.¹ Although researchers have used data from the MSRE in the past to assess results from simulations, up to this time, no official benchmark was available in “The 2019 Edition of the IRPhEP Handbook”² (hereinafter referred to as the IRPhEP Handbook). The scope of the International Reactor Physics Experiment Evaluation Project (IRPhEP) is to collect standardized reactor physics benchmark data sets of the highest quality as certified by a group of international experts that peer-reviews each set. In order to fill the gap in the IRPhEP, the University of California, Berkeley (UC Berkeley), and ORNL have joined forces to retrieve information from the MSRE and to create the first MSR-related benchmark that appeared in the IRPhEP Handbook.

This paper documents the steps and the assumptions made in the process of creating a benchmark model of the MSRE first criticality experiment with ^{235}U fuel, conducted in June 1965 (Ref. 3). A description of the MSRE and the

*E-mail: maxfratoni@berkeley.edu

This is an Open Access article distributed under the terms of the Creative Commons Attribution-NonCommercial-NoDerivatives License (<http://creativecommons.org/licenses/by-nc-nd/4.0/>), which permits non-commercial re-use, distribution, and reproduction in any medium, provided the original work is properly cited, and is not altered, transformed, or built upon in any way.

procedure that was followed to achieve criticality are provided in Secs. II and III, respectively. Section IV describes the benchmark model, and Sec. V reports the results obtained from numerical simulations of the model.

II. MSRE DESCRIPTION

The MSRE was a molten salt liquid fuel critical facility operated at ORNL from 1965 to 1969. As the first large-scale, long-term, high-temperature testing performed for a fluid fuel salt, a graphite moderator, and a then-new nickel-based alloy (named INOR-8) in a reactor environment, the MSRE purpose was to demonstrate key features of the molten salt liquid fuel concept and to prove the practicality of the MSR technology.¹ The MSRE primary system included a reactor vessel, a fuel circulating pump, a fuel heat exchanger, and an interconnecting piping. Fuel-bearing salt circulated through these components at an average nominal rate of $4.54 \text{ m}^3/\text{min}$ achieving criticality and heating up in the reactor core. The primary system was housed in a carbon steel vessel named the reactor cell. The reactor vessel was further confined within a thermal shield structure. This section provides a brief description of the geometry, dimensions, and materials of the reactor core, vessel, and thermal shield (more detailed information can be found in Ref. 1). Components outside of the thermal shield were believed to have no impact on the benchmark and were not considered.

II.A. Reactor Vessel

A cutaway drawing of the MSRE reactor vessel is shown in Fig. 1. The reactor vessel has an inner diameter of 147.32 cm and a height of 233.90 cm. The fuel salt enters the flow distributor through the fuel inlet, arranged tangentially to the top of the vessel. The flow distributor is half-circular in cross section with an inside radius of 10.16 cm. The fuel is distributed evenly around the circumference of the vessel while passing the flow distributor and then flows turbulently downward in a spiral path through a 2.54-cm-wide annulus between the vessel wall and the core can. The salt loses its rotational motion in the 48 straightening vanes in the lower plenum and flows upward through the graphite matrix in the core can. The vessel has two torispherical domes with 147.32-cm inner diameter and 2.54-cm thickness as the upper plenum and lower plenum. The core can inside the vessel has an inner diameter of 140.97 cm and a thickness of 0.635 cm. The core can is supported—and also held down when salt is in the reactor—by a ring at the top that is bolted to 36 lugs

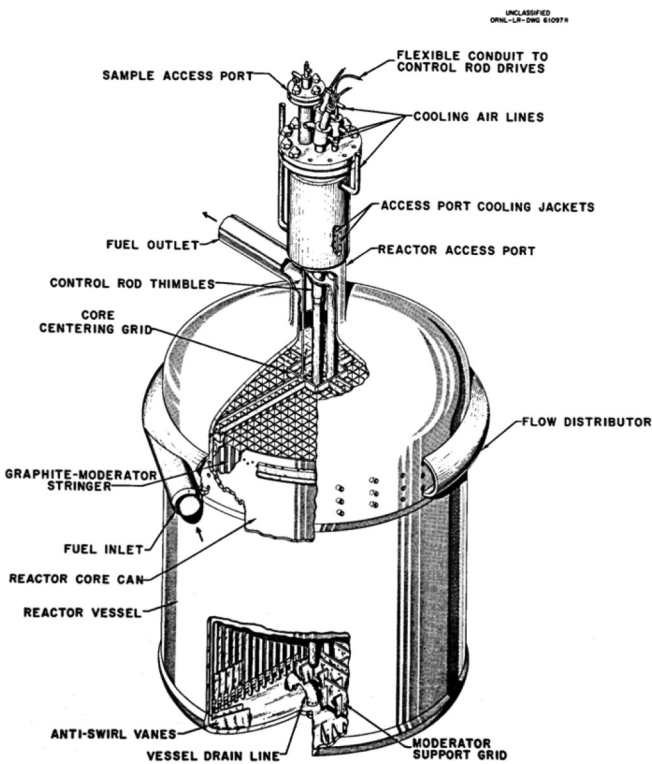


Fig. 1. MSRE reactor vessel.¹

welded to the inside wall of the reactor vessel. The can, in turn, supports the graphite in the reactor.¹

II.B. Reactor Core

The reactor core structure is an assembly of vertical graphite stringers with a $5.08 \times 5.08\text{-cm}$ cross section as shown in Fig. 2. Fissioning occurs when the fuel salt flows through the channels formed by grooves in the four sides on the stringers. These channels are $1.016 \times 3.048\text{ cm}$ with round corners of radius 5.08 cm. The graphite stringers are 170.03 cm long and are mounted in a vertical close-packed array. There is a total of 1140 equivalent full-size passages, counting fractional sizes. The dimensions of the flow channel provide a large enough passage to avoid blockage by small pieces of graphite and correspond to a nearly optimum fuel-to-graphite ratio in the core.

The MSRE graphite has an average density of 1.86 g/cm^3 , which is lighter than the salt density, which is approximately 2.3275 g/cm^3 . When not buoyed up by being immersed in the fuel salt, the vertical graphite stringers rest on a lattice of graphite blocks, with a $2.54 \times 4.1275\text{-cm}$ cross section, that is laid horizontally in two layers at right angles to each other. Holes in the

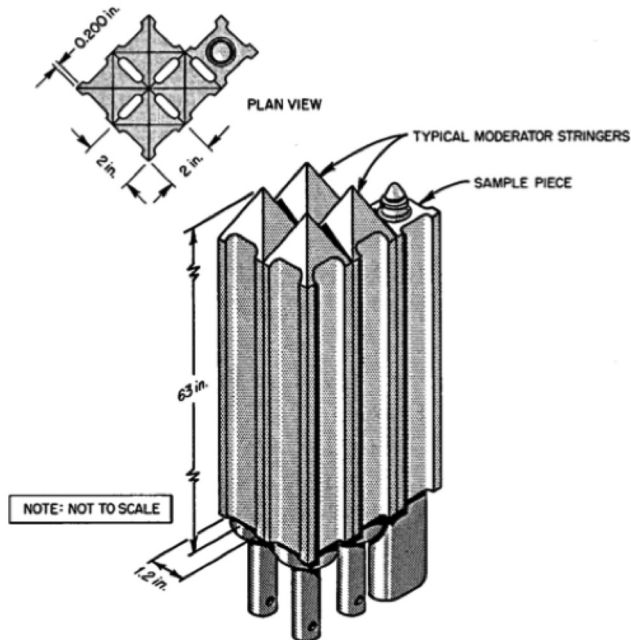


Fig. 2. Graphite stringers and their arrangement in the MSRE core.¹

lattice blocks (2.642-cm diameter) house the 2.54-cm-diameter doweled section at the lower end of each stringer. The upper horizontal surface of the vertical graphite stringers is tapered to ensure that no salt remains on it after drainage (Fig. 2).

II.C. Control Rod and Sample Basket

Four channels, three hosting control rod thimbles and one hosting baskets containing graphite and INOR-8 samples, are arranged equidistantly near the center of the core in place of four graphite stringers, as shown in Fig. 3. One of the objectives of the MSRE was to investigate the behavior of bare graphite in the reactor environment. Thus, the reactor was designed for periodic removal of graphite specimens from the sample baskets near the center of the core. There are three identical sample baskets mounted vertically, and each basket features a 0.079-cm-thick INOR-8 plate and 0.238-cm-diameter holes and contains four samples (0.635 cm in diameter and 167.64 cm in length) of INOR-8 and five samples of graphite (0.635 × 1.1938 cm with a length of 167.64 cm).

The control rod thimbles have a wall tubing of 5.08-cm outer diameter and 0.1651-cm thickness. The control rods are segmented (see Fig. 4) to provide the flexibility needed to pass through the bends in the control rod thimbles. The poison material is in the form of thin-

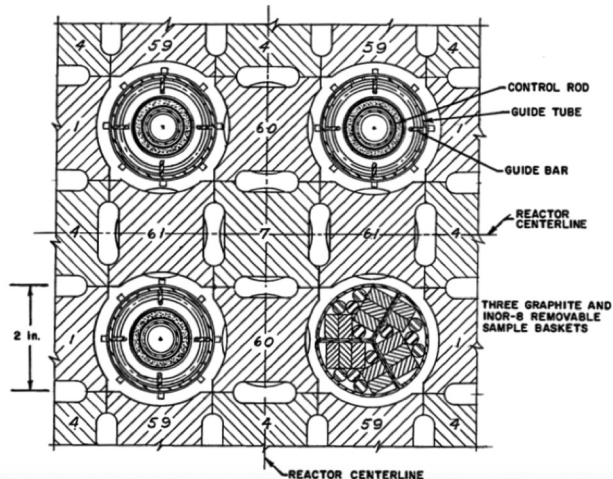


Fig. 3. Control rod and sample basket layout at the center of the core.¹

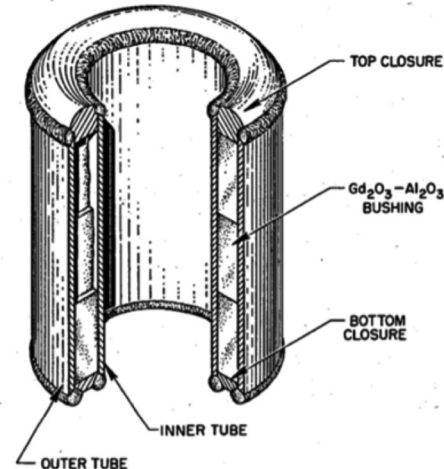


Fig. 4. Cutaway of an MSRE control element.¹

walled, ceramic cylinders, and the ceramic cylinder is a mixture of 70 wt% Gd_2O_3 and 30 wt% Al_2O_3 . Each control element contains three ceramic cylinders, canned in an Inconel shell. Each control rod is made of 38 elements for a total length of the poison section of 150.774 cm. The segments are threaded, beadlike, on a 1.905-cm outer diameter × 1.5875-cm inner diameter helically wound, flexible stainless steel. Two 0.3175-cm-diameter braided Inconel cables run through this hose to restrain it from stretching when dropped in free fall. This hose passes upward through the thimble to the positioning chain on the control rod drive mechanism. The reference system used to determine control rod position is shown in Fig. 5. In this system, zero corresponds to a fully inserted rod when driven in whereas a fully withdrawn rod is positioned at 51 in.

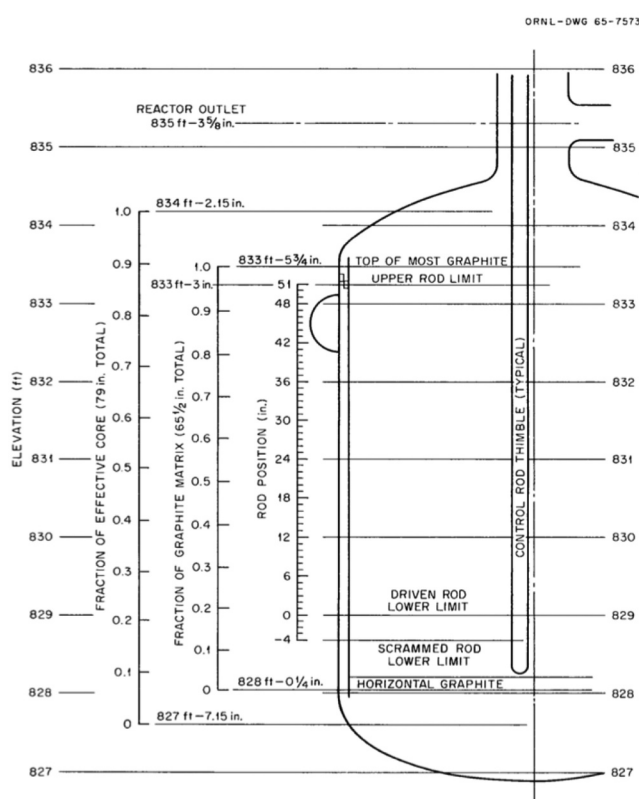


Fig. 5. Elevations of core components and control rod position reference system.³

II.D. Thermal Shield

The reactor vessel is installed in a Type 304 stainless steel thermal shield that supports the vessel and forms the outer wall of the reactor furnace. The shield has an approximate outer diameter of 317.5 cm, an inner diameter of 236.22 cm, and a height of 383.54 cm. The inside of the thermal shield is lined with 15.24 cm of high-temperature insulation (vermiculite). The reactor vessel is supported from the top removable cover of the thermal shield.

III. FIRST CRITICALITY EXPERIMENT

In 1965, a first criticality experiment was conducted at the MSRE with the purpose of establishing the critical concentration of ^{235}U under the simplest possible conditions, that is, isothermal core, stationary fuel salt, and fully withdrawn control rods. To start, carrier salt (65LiF-30BeF₂-5ZrF₄) and depleted uranium eutectic (73LiF-27UF₄) were loaded in the drain tanks and circulated in the primary loop for 10 days. Then, increments of enriched uranium concentrate (93% ^{235}U) were

progressively added to the salt, and the approach to critical concentration was monitored by measuring neutron source multiplication. At first, kilogram quantities of ^{235}U were added to the salt in the drain tanks. Then, the salt was transferred to the core, and the neutron multiplication was measured. This process was repeated until the salt contained approximately 98% in weight of the anticipated critical mass. The remainder ^{235}U was added in 85-g batches through the sampler-enricher. Four neutron counting channels were used during the experiment: two fission chambers in the instrument shaft, a BF₃ chamber in the instrument shaft, and another BF₃ chamber in the thermal shield.

On June 1, 1965, at approximately 6:00 p.m., the reactor reached the critical point with fuel salt stationary, two rods at fully withdrawn position (51 in.) and the other rod inserted at 3% of its integral worth (46.6 in.) (Ref. 3). Criticality was verified by leveling the power at a successively higher level with the same rod position. The actual system power was approximately 10 W. The corrected value of the book mass fraction of ^{235}U in the fuel salt was (1.408 ± 0.007) wt% considering the small amount of dilution of the fuel salt from residues of flush salt left in freeze valves and drain tank heels when the fuel salt was charged. The core temperature at the time of criticality was 911 K (1181°F) instead of 922 K (1200°F) as initially estimated. The fuel salt density was 2.3275 ± 0.0160 g/cm³, and its composition was 64.88 mol % LiF, 29.27 mol % BeF₂, 5.06 mol % ZrF₄, and 0.79 mol % UF₄.

IV. BENCHMARK MODEL

A high-fidelity benchmark model of the MSRE was created with the ultimate purpose of validating computational tools. Figures 6 and 7 provide an overview of the model, including axial location with respect to the bottom of the horizontal graphite lattice and radial dimensions. The arrangement of the graphite stringers is disrupted in the center by three control rods and the sample baskets as shown in Fig. 8. Additional disruption to the pattern of the stringers occurs at the outer edge where partial stringers and partial channels are used and in the center of the core where stringers are shorter. For brevity, these and other details are not reported here, and readers interested in recreating the benchmark model should refer to Ref. 2 or Ref. 4 for a complete description.

The dimensions and materials for the horizontal and vertical graphite lattices, control rod thimbles, sample baskets, reactor vessel shell, flow distributor, and thermal

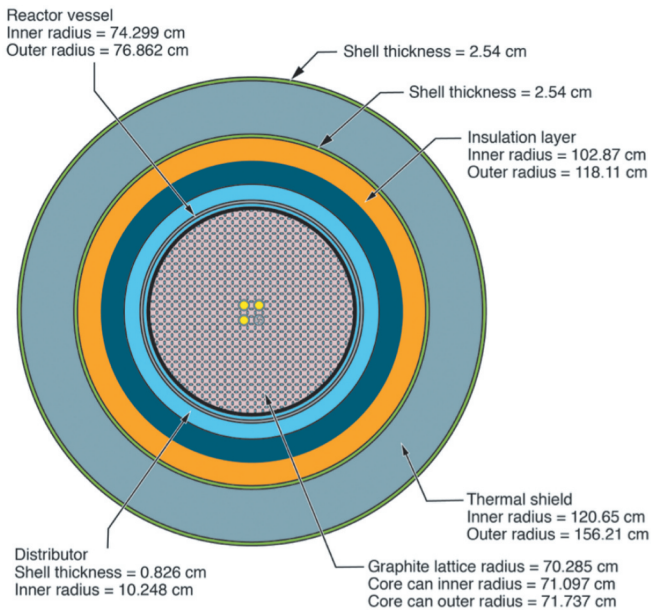


Fig. 6. Horizontal cross section of the MSRE model at 911 K. The cross section is located at the centerline of the flow distributor ($z = 145.396$ cm in Fig. 7). Image credit: David R. Sharp, Idaho National Laboratory.

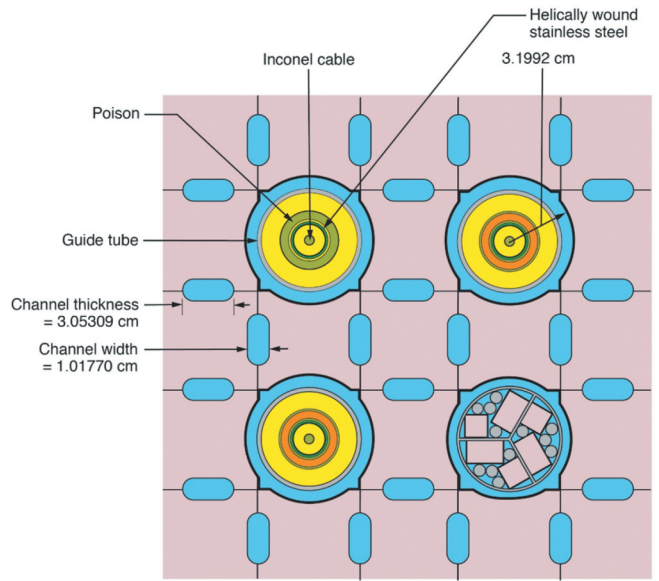


Fig. 8. Horizontal cross section of the core center with control rods and sample baskets. Image credit: David R. Sharp, Idaho National Laboratory.

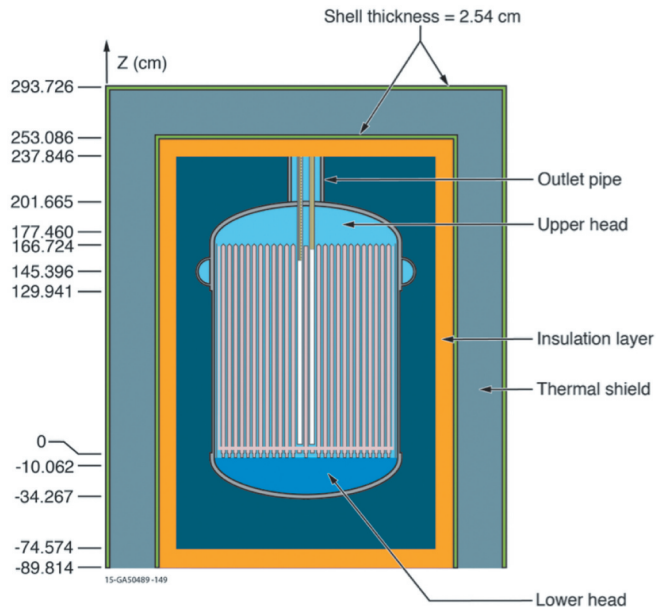


Fig. 7. Vertical cross section of the MSRE model at 911 K. The cross section is offset by 5.08339 cm from the center of the graphite stinger lattice in order to show control rods. Location $z = 0$ corresponds to the bottom of the horizontal graphite lattice. Image credit: David R. Sharp, Idaho National Laboratory.

shield are those obtained from design data and blueprints as reported in Sec. II. The fuel inlet pipe, fuel outlet pipe, fuel outlet strainer, reactor access port, external loop outside the thermal shield, and base for the thermal shield

were neglected. The bias from neglecting these components in the benchmark was evaluated by creating a fully detailed model (Fig. 9) that contains the fuel inlet pipe, fuel outlet pipe, fuel outlet strainer, reactor access port, and thermal shield base, and the bias on k_{eff} was calculated to be (-22 ± 5) pcm.

There are other simplifications in the MSRE benchmark model that are believed to have no significant effect on k_{eff} . The lower head of the reactor vessel is simplified as a homogeneous mixture of fuel salt and INOR-8 with a volume ratio of 90.8:9.2 according to Ref. 5. The upper head of the reactor vessel is simplified as a pure salt region. The insulation layer and thermal shield are also simplified as a homogeneous mixture.

The dimensions reported in the design documents and in the blueprints are as built, thus at room temperature. During the critical experiment the registered temperature was 911 K; therefore, dimensional changes to graphite and metallic components in the reactor vessel were applied assuming a thermal expansion coefficient of $1.5 \times 10^{-6}^{\circ}\text{F}^{-1}$ for graphite and of $7.8 \times 10^{-6}^{\circ}\text{F}^{-1}$ for metallic components.⁶ It was assumed that the reactor vessel freely expanded downward starting from the interface between the outlet pipe and the upper insulation layer. The horizontal graphite lattice was connected to the vessel at its bottom ($z = 0$ in Fig. 7), and the vertical graphite stringers were held by the horizontal graphite lattice; therefore, to account for thermal expansion, the horizontal graphite lattice was first moved together with

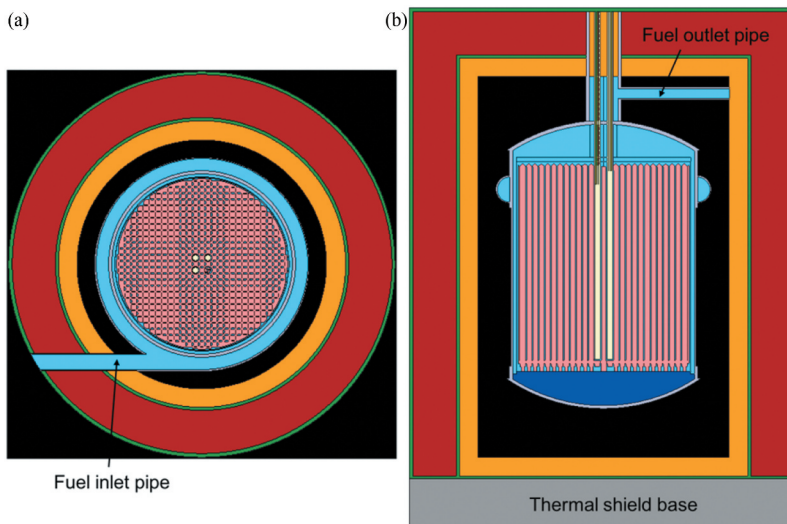


Fig. 9. (a) Horizontal cross section at $z = 145.396$ cm and (b) vertical cross section of the core offset by 5.08339 cm from the center of the fully detailed MSRE model.

the vessel and then thermally expanded upward. Finally, the thermally expanded vertical graphite stringers were placed above the horizontal graphite lattice. Table I reports hot and cold dimensions.

V. RESULTS

The benchmark model was simulated using the Monte Carlo neutron transport code Serpent 2 version 2.1.30 (Ref. 7) with the ENDF/B-VII.1 cross-section library. The temperature for cross sections was set at 900 K, and it was preprocessed for Doppler broadening to 911 K by Serpent 2. Thermal scattering laws were applied to carbon in graphite (with a temperature of 911 K in the core and 305 K in the thermal shield) and

hydrogen in water (with a temperature of 305 K in the thermal shield). For the thermal scattering laws, Serpent 2 interpolates between the two closest available temperature libraries.

The experimental k_{eff} is 1.0, and the assessed bias of the benchmark model from simplifications is -22 pcm; thus, the expected k_{eff} for the benchmark model is $0.99978, \pm 420$ pcm uncertainty as reported below. The k_{eff} calculated by Serpent is 1.02132 ± 0.00003 , which is 2.154% larger than the experimental and the benchmark model values. The complexity of the model and the fact that it was reconstructed more than 50 years after the experiment based on the publicly available documents make it difficult to identify the source(s) of such discrepancy. It can be noticed that k_{eff} is particularly sensitive, as expected, to the main core components, which are salt

TABLE I
As-Built Cold Dimensions and Thermally Expanded Hot Dimensions

Dimension	Cold (293 K)	Hot (911 K)
Graphite lattice radius (cm)	70.168	70.285
Core can inner radius (cm)	70.485	71.097
Core can outer radius (cm)	71.120	71.737
Reactor vessel inner radius (cm)	73.660	74.299
Reactor vessel outer radius (cm)	76.200	76.862
Graphite stringer width (cm)	5.075	5.084
Fuel channel width (cm)	1.016	1.018
Fuel channel length (cm)	3.048	3.053
Graphite stringer height (cm)	170.027	170.311
Total height of the vessel (cm)	269.771	272.113
Length of the control rod inserted (cm)	76.414	77.077

and graphite. The salt composition is particularly challenging to determine as obtained by successive additions of different compositions, and changes in salt composition would largely impact k_{eff} (further details are discussed later in this section). At the time the benchmark was prepared, thermal scattering kernel data for salt were not available, although the impact of that is likely to be much smaller than the observed difference.

The impact of the nuclear data was evaluated comparing the ENDF/B-VII.1 and JENDL-4.0 cross-section libraries. The difference in k_{eff} between the two is (71 ± 5) pcm (Table II). In addition, the eigenvalue for the MSRE core calculated using the ENDF/B-VII.1 data is (178 ± 5) pcm lower if only the carbon cross section is replaced with JENDL-4.0 data. The difference in k_{eff} between the two is (71 ± 5) pcm (Table II). In addition, the eigenvalue for the MSRE core calculated using ENDF/B-VII.1 data is (178 ± 5) pcm lower if only the carbon cross section is replaced with JENDL-4.0 data.

It is also observed that other benchmarks of graphite-moderated systems currently included in the IRPhEP

Handbook report calculated k_{eff} 1% to 2% larger than the experimental value as shown in Table III. Such discrepancy is possibly due to uncertainties in the impurity content of graphite or to the accuracy of the neutron capture cross section of carbon.

V.A. Experimental and Data Uncertainties

All input data to the benchmark model are characterized by their own uncertainty that propagates to the multiplication factor. In order to assess this uncertainty, k_{eff} was calculated perturbing each parameter i within its uncertainty range, in both positive and negative directions, and the corresponding Δk_i was determined as follows:

$$\Delta k_i = \frac{u_i}{\delta x_i} (k_{\delta_i} - k_{ref}) , \quad (1)$$

where u_i is the standard uncertainty of parameter i and $(k_{\delta_i} - k_{ref})$ is the change in k_{eff} induced by change δx_i on parameter i . When there was a difference between the absolute values of Δk_i calculated from the positive

TABLE II
Expected and Calculated Benchmark Model k_{eff} Values

Case	k_{eff}	100 (C-E)/E ^a
Benchmark	0.99978 ± 0.00420	—
SERPENT, ENDF/B-VII.1	1.02132 ± 0.00003	2.154
SERPENT, JENDL-4.0	1.02061 ± 0.00003	2.083

^aC = calculated value. E = experimental value.

TABLE III
Difference Between Calculated and Expected k_{eff} for Selected Full-Core Benchmarks of Carbon-Moderated Systems Included in the IRPhEP Handbook*

Benchmark Model	Code Library	Expected k_{eff}	Calculated k_{eff}	100 (C-E)/E ^a
HTR10 high-fidelity	MCNP5 ENDF/B-VI	1.0000	1.01190 ± 0.00021	1.19
HTR10 simplified	MCNP5 ENDF/B-VI	1.0131	1.02500 ± 0.00021	1.18
HTTR fully loaded	MCNP5 ENDF/B-VII.0	1.0025	1.02310 ± 0.00010	2.03
PROTEUS Core 3	MCNP5 ENDF/B-VII.0	0.9999	1.00888 ± 0.00007	0.90

*Reference 2.

^aC = calculated value. E = experimental value.

TABLE IV
Individual and Total Uncertainties on k_{eff}

Item	Nominal and Bounding Values	Δk_i (pcm)
Graphite density	1.86, 1.83 to 1.87 g/cm ³	334
Fuel salt density	(2.3275 ± 0.0160) g/cm ³	103
Be mass in carrier salt	(309.62 ± 5.00) kg	8
Zr mass in carrier salt	(541.36 ± 5.00) kg	12
235U mass fraction in the salt	(1.409 ± 0.007) wt%	81
234U mass fraction in the salt	(0.014 ± 0.007) wt%	74
236U mass fraction in the salt	(0.006 ± 0.006) wt%	17
INOR-8 density	(8.7745 ± 0.0200) g/cm ³	3
Graphite core height	(166.724 ± 1.000) cm	21
Graphite core radius	(70.285 ± 0.200) cm	4
Fuel channel width	(1.0160 ± 0.0127) cm	51
Fuel channel length	(3.0480 ± 0.0127) cm	23
^{6}Li enrichment	(0.005 ± 0.001) at. %	172
Boron concentration in graphite	(0.000 080 ± 0.000 008) wt%	17
Temperature of thermal shield	305 K, 600 K	2
Temperature of fuel salt	(911 ± 1) K	6
Temperature of graphite	(911 ± 1) K	1
Height vertical section of bottom head	(6.475 ± 1.000) cm	9
Outlet pipe thickness	(2.511 ± 0.250) cm	3
Outlet pipe height	(36.180 ± 1.000) cm	4
Distributor thickness	(0.826 ± 0.080) cm	3
Sample basket outer diameter	(5.4287 ± 0.0127) cm	0.0
Sample basket gap	0, 0.0127 cm	5
Cell atmosphere gas composition	Mass fraction versus atom fraction	0.0
INOR-8 composition (C mass fraction)	0.06%, 0.08%	5
Mo mass fraction in INOR-8	(17.0 ± 0.5) wt%	12
Cr mass fraction in INOR-8	(7.0 ± 0.5) wt%	5
Fe mass fraction in INOR-8	(5.0 ± 0.5) wt%	4
Impurities in salt	Fe: 162 ± 65 ppm, Cr: 28 ± 7 ppm Ni: 30 ± 20 ppm, O: 490 ± 49 ppm	12
Helium void in salt	0, 0.076 vol %	5
Salt absorption in graphite	0, 0.0010 vol %	2
Hf in Zr	50 ppm, 0 ppm	12
Impurities in graphite	Ash: (0.00050 ± 0.00005) wt% V: (0.00090 ± 0.00009) wt% S: (0.00050 ± 0.00005) wt%	4
Graphite stringer width	(5.07492 ^{+0.0000} _{-0.0127}) cm	13
Poison density	(5.873 ± 0.020) g/cm ³	0.5
Gd ₂ O ₃ mass fraction	(70 ± 1) wt%	0.6
Control rod position	(118.364 ± 0.127) cm	0.7
Regulating rod	Rod 1, rod 2, or rod 3	0.0
Graphite thermal expansion coefficient	(1.5 ± 0.2) × 10 ⁻⁶ °F ⁻¹	18
INOR-8 thermal expansion coefficient	(7.8 ± 0.2) × 10 ⁻⁶ °F ⁻¹	17
Measurement uncertainty in k_{eff}	—	10
Total (root-mean-square)	—	420

and negative perturbations of a parameter, the larger one was selected and shown in Table IV. For this evaluation, all the parameters were considered uncorrelated, and the total standard uncertainty of k_{eff} was calculated as the root-mean-square of all Δk_i .

The (1 σ) uncertainty of the experimental k_{eff} is 420 pcm, as shown in Table IV. Graphite density, fuel salt density, and ^{6}Li enrichment are the main contributors.

The effect of the temperature of the thermal scattering data was evaluated as shown in Table V. It was found

TABLE V
Comparison of k_{eff} with Various Thermal Scattering Cross-Section Temperatures

Carbon in Graphite	Carbon in Thermal Shield	Hydrogen in Thermal Shield	k_{eff}	Difference (pcm)
800 K	296 K	293.6 K	1.02723 ± 0.00010	591
911 K ^a	305 K ^a	305 K ^a	1.02132 ± 0.00003	0
1000 K	400 K	350 K	1.01640 ± 0.00010	-492

^aThermal scattering cross section interpolated by Serpent based on available data at 800 K and 1000 K.

that a 100 K change in the temperature of the thermal scattering data of carbon in graphite results in more than 500 pcm difference in k_{eff} ; therefore, the use of an accurate temperature library is recommended.

The salt composition used in the benchmark model, reported in Ref. 8, was obtained recording the amount and the composition of each salt addition into the primary loop and was checked and corrected by the experimenters to be self-consistent. Nevertheless, Ref. 8 reports two additional salt compositions. One was obtained from chemical and mass spectroscopy analysis at the time of criticality, and the other was the anticipated composition with no correction. The effect on k_{eff} of these alternative compositions was evaluated keeping throughout the same enrichment of all uranium isotopes, the same impurity concentration, and the same total salt density (Table VI). It was found that the results from chemical analysis show bias in the determination of lithium and beryllium concentrations. Such measurement bias from the chemical analysis was noticed on the flush salt.⁸ Flush salt was used initially to flush the system before loading fuel salt and later on before and after maintenance periods. The nominal composition of the flush salt was LiF-BeF₂ (66 to 34 mol %); however, the composition determined by chemical analysis was LiF-BeF₂ (63.560 ± 0.005) mol % to (36.440 ± 0.005) mol %. The anticipated composition is very similar to the one selected for the benchmark, but

the latter provides the best agreement with the recorded ²³⁵U mass fraction: 1.409% versus (1.408 ± 0.007)% recorded.³ Such metric is considered the most reliable as the overall scope of the experiment was to determine the critical amount of ²³⁵U.

Sensitivity coefficients of k_{eff} to uncertainties in the nuclear data (Table VII) were calculated using Serpent 2 (Ref. 9), and the uncertainty on k_{eff} due to the cross-section data was estimated combining the sensitivity coefficients with covariance data [56-group covariance matrices were obtained from SCALE 6.2 (Ref. 10)] through the so-called sandwich rule. The total uncertainty was estimated to be 664 pcm, and the most important uncertainty contributors are listed in Table VIII.

V.B. Simplified Model

Given the complexity of the MSRE model, it might be challenging for some reactor physics codes to reproduce the benchmark model in full details; therefore, reference k_{eff} values were also computed for models with various simplifications:

1. The half-torus flow distributor, located at the top of the vessel connecting the fuel salt inlet, was removed (Fig. 10).

TABLE VI
Comparison of k_{eff} with Different Fuel Salt Compositions*

Salt Composition	Lithium (wt%)	Beryllium (wt%)	Zirconium (wt%)	Uranium (wt%)	Fluorine (wt%)	k_{eff}
Benchmark	10.957	6.349	11.101	4.495	67.027	1.02132 ± 0.00003
Chemical analysis	10.327	6.695	11.016	4.440	67.451	1.02248 ± 0.00010
Anticipated	10.970	6.324	10.972	4.641	67.023	1.02595 ± 0.00010

*0.071 wt% impurities in all cases.

TABLE VII
Sensitivity Coefficients for k_{eff} from Cross-Section Data Uncertainties

Nuclide	Total ($\times 10^{-5}$)	Elastic Scattering ($\times 10^{-5}$)	Neutron Capture ^a ($\times 10^{-5}$)	Fission ($\times 10^{-5}$)
${}^6\text{Li}$	-1430	0.04	-1430	—
${}^7\text{Li}$	770	2010	-1380	—
${}^9\text{Be}$	2920	3250	-340	—
${}^{90}\text{Zr}$	3	50	-64	—
${}^{91}\text{Zr}$	-520	150	-670	—
${}^{92}\text{Zr}$	-16	130	-160	—
${}^{94}\text{Zr}$	-36	5	-54	—
${}^{96}\text{Zr}$	-86	2	-89	—
${}^{19}\text{F}$	8410	8080	-1070	—
${}^{nat}\text{C}$	51 400	39 210	-1760	—
${}^{10}\text{B}$	-650	0.2	-650	—
${}^{235}\text{U}$	22 990	47	-14 080	37 020
${}^{238}\text{U}$	-8470	610	-9170	63

^aAs defined in Serpent includes all reactions with no neutron yield.

TABLE VIII
Uncertainties on k_{eff} due to Cross-Section Data Uncertainties

Reaction	Uncertainties (pcm)
${}^{235}\text{U}, \bar{\nu}$	373
Carbon, elastic	264
${}^{235}\text{U}, \chi$	257
${}^7\text{Li}(n,\gamma)$	197
${}^{235}\text{U}(n,\gamma)$	172
${}^{19}\text{F}$ elastic	150
$\times {}^{235}\text{U}(n,\gamma)$	128
${}^{235}\text{U}(n,f)$	120
${}^{58}\text{Ni}(n,\gamma)$	97
${}^{19}\text{F}$ inelastic	96

2. The top and bottom heads of the reactor vessel were assumed flat rather than torispherical domes, and the total height of the vessel was conserved (Fig. 11).

3. The sample baskets were removed, and the housing channel was filled with graphite (Fig. 12b).

4. Materials in the sample basket were homogenized while the basket outer radius and the channel shape were kept unchanged (Fig. 12c).

5. Salt channels in between stringers were modeled as circular with 0.957-cm radius in order to maintain the same cross-sectional area as the reference channels (Fig. 13b).



Fig. 10. Vertical cross section of the MSRE model without the distributor (at $y = 0$).

6. Salt channels in between stringers were modeled as rectangular channels (Fig. 13c) with the long side equal to the length of the long side of the reference

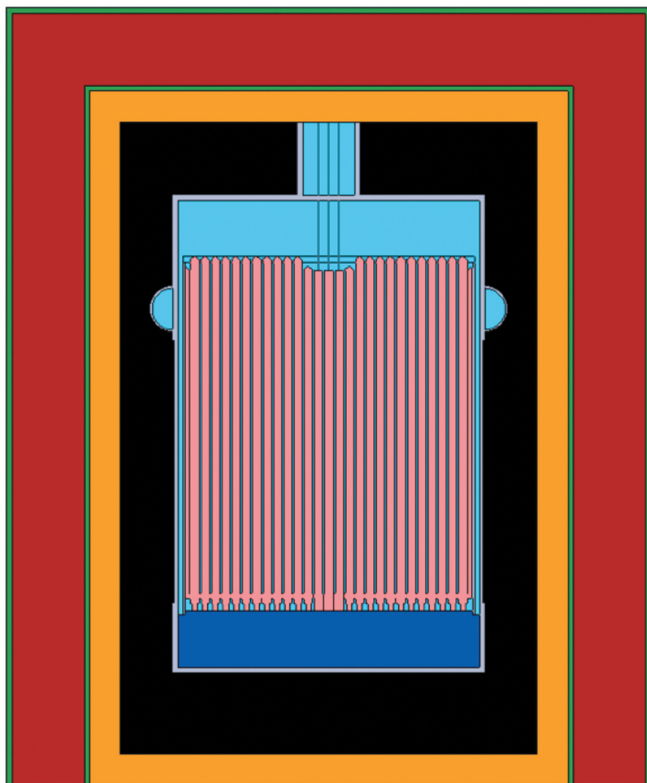


Fig. 11. Vertical cross section of the MSRE model with flat top and bottom sections (at $y = 0$).

channels (3.048 cm) and the half-length of the short side (0.472 cm) adjusted to preserve the channel cross-sectional area.

7. The thermal shield and insulation layer were removed from the model (see Fig. 14).

Table IX reports the calculated k_{eff} for the simplified models illustrated above.

VI. CONCLUSIONS

This paper documents the effort of developing a high-quality reactor physics benchmark for the MSRE that has been reviewed and approved by the IRPhEP committee to be included in the IRPhEP Handbook. A highly detailed benchmark model of the MSRE was created collecting data from publicly available documents written both before and after the facility was operated. In particular, the benchmark aimed at reproducing the first criticality experiment with ^{235}U fuel, conducted at zero power with stationary salt and uniform temperature. Blueprints and design documents provided an abundance of information to build a model; nevertheless, it was not possible to establish if any change was made during

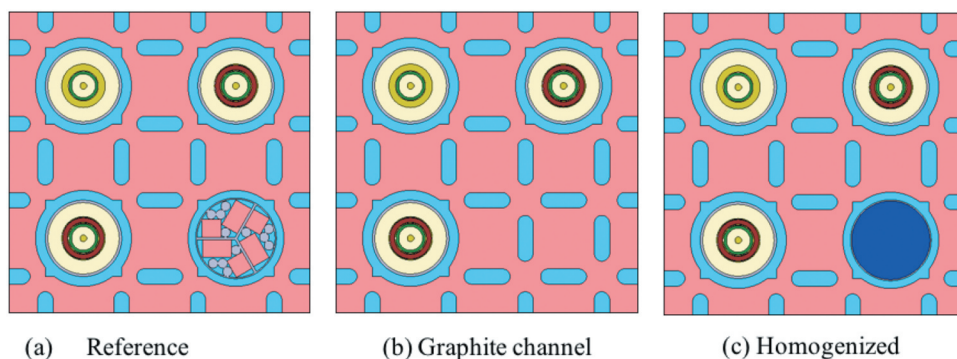


Fig. 12. Comparison of models for the sample basket.

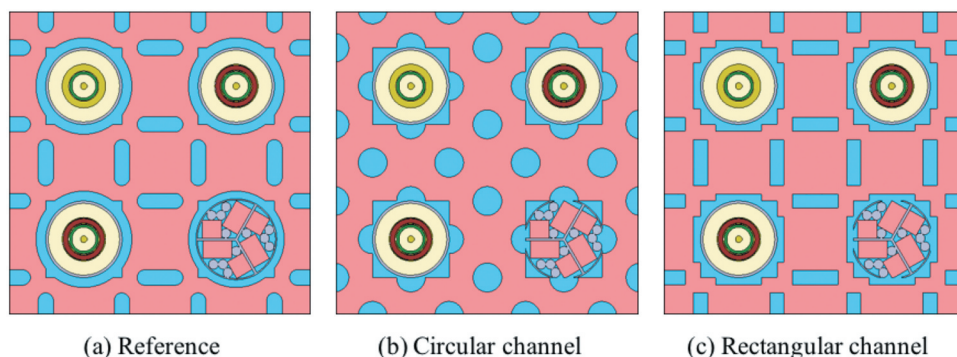


Fig. 13. Comparison of models for the fuel channel.

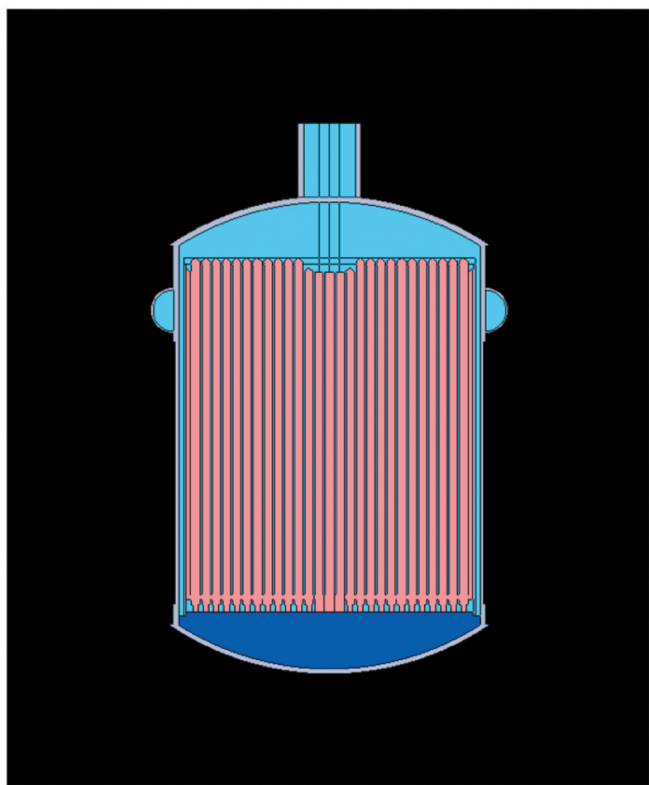


Fig. 14. Vertical cross section of the MSRE model without thermal shield and insulation layer (at $y = 0$).

TABLE IX
Calculated k_{eff} with Various Model Simplifications

Case	k_{eff}	$100(k_{eff} - k_{ref})/k_{ref}$ ^a
No distributor	1.02032 ± 0.00004	-0.098
Flat top and bottom heads	1.02380 ± 0.00004	0.243
Sample baskets replaced with graphite	1.03790 ± 0.00004	1.623
Homogeneous sample baskets	1.02094 ± 0.00003	-0.037
Circular fuel channels	1.02450 ± 0.00003	0.311
Rectangular fuel channel	1.02151 ± 0.00004	0.019
No thermal shield and insulation layer	1.01228 ± 0.00003	-0.885

^a $k_{ref} = 1.02132 \pm 0.00003$.

actual construction. Furthermore, the documented dimensions are “as built” that is at room temperature, but at the moment of criticality, a uniform temperature of 911 K

was recorded. In the benchmark model, the best effort was made to account for thermal expansion. Salt composition is largely documented, and some discrepancies exist and are even noted in documents of the time. Such a parameter is of the greatest impact on reactor physics, and once again, the best effort was made to reconstruct the salt composition guided by the fact that the ^{235}U concentration was expected to be accurately reported as the main target of the criticality experiment.

The benchmark model was simulated using the Monte Carlo code Serpent 2 with the nuclear data library ENDF/B-VII.1 in order to calculate the neutron multiplication factor as well as bias and uncertainties related to the model. It was estimated that the benchmark bias on k_{eff} , the error due to approximations in the model, is as little as (-22 ± 5) pcm whereas the uncertainty due to uncertainties in the input parameters, i.e., tolerance, is 420 pcm. The computed multiplication factor is 2.154% higher than the experimental one, which is a 5σ difference. The reason for such difference was difficulty in tracking; nevertheless, it was observed that similar large differences are reported in other benchmarks for graphite-moderated systems that appear in the IRPhEP Handbook. This might indicate that further investigation is needed into graphite composition and carbon nuclear data.

This benchmark model provides the foundation to extend MSRE benchmarks beyond multiplication factor and to include other quantities of interest such as reactivity coefficients, control rod worth, reactivity impact of salt motion, etc. An effort in this direction is already ongoing based on the experiments that followed the first criticality. Future work should extend benchmark efforts beyond zero-power operation and potentially to ^{233}U -bearing salt. All such experiments have been conducted at the MSRE, although the accuracy and the level of details reported in publicly available documents remain to be assessed.

Acknowledgments

The authors express the deepest gratitude to those who greatly contributed to improve the quality of this benchmark, in particular, the IRPhEP external reviewers Luka Snoj (Jozef Stefan Institute) and Aslak Stubsgaard (Copenhagen Atomics), the chair of the IRPhEP expert group John Bess (Idaho National Laboratory), and all the members of IRPhEP. This research used the Savio computational cluster resource provided by the Berkeley Research Computing program at UC Berkeley

(supported by the UC Berkeley Chancellor, Vice Chancellor for Research, and Chief Information Officer). This research was performed using funding received from the U.S. Department of Energy Office of Nuclear Energy's Nuclear Energy University Programs.

ORCID

Massimiliano Fratoni  <http://orcid.org/0000-0003-0452-0508>

References

1. R. C. ROBERTSON, "MSRE Design and Operations Report Part I: Description of Reactor Design," ORNL-TM -0728," Oak Ridge National Laboratory (1965).
2. J. D. BESS et al., "The 2019 Edition of the IRPhEP Handbook," INL/CON-19-53745-Rev000, Idaho National Laboratory (Oct. 2019).
3. B. E. PRINCE et al., "Zero-Power Physics Experiments on the Molten-Salt Reactor Experiment," ORNL-4233," Oak Ridge National Laboratory (1968).
4. M. FRATONI et al., "Molten Salt Reactor Experiment Benchmark Evaluation," DOE-UCB-8542, University of California, Berkeley (Mar. 2020).
5. P. N. HAUBENREICH et al., "MSRE Design and Operations Report Part III: Nuclear Analysis," ORNL-TM -730," Oak Ridge National Laboratory (1964).
6. R. C. ROBERTSON, "MSRE Design and Operations Report Part I: Description of Reactor Design," ORNL-TM -728, Oak Ridge National Laboratory (1965).
7. J. LEPPANEN et al., "The Serpent Monte Carlo Code: Status, Development and Applications in 2013," *Ann. Nucl. Energy*, **82**, 142 (2015); <https://doi.org/10.1016/j.anucene.2014.08.024>.
8. R. E. THOMA, "Chemical Aspects of MSRE Operation," ORNL-4658, Oak Ridge National Laboratory (1971).
9. M. AUFIERO et al., "A Collision History-Based Approach to Sensitivity/Perturbation Calculations in the Continuous Energy Monte Carlo Code Serpent," *Ann. Nucl. Energy*, **85**, 245 (2015); <https://doi.org/10.1016/j.anucene.2015.05.008>.
10. W. A. WIESELQUIST, R. A. LEFEBVRE, and M. A. JESSEE, "SCALE Code System," ORNL/TM-2005/39, Version 6.2.4, Oak Ridge National Laboratory (2020).